AGU PUBLICATIONS

JGR

Journal of Geophysical Research: Biogeosciences

RESEARCH ARTICLE
10.1002/2017JG003907

Key Points:
- Carbon chemistry was influenced by riverine freshwater and ice-melting
- Ice melting drives low alkalinity in surface seawater
- High pCO_2 and low Ω_{arag} due to ice melting might influence to marine calcifiers

Correspondence to:
C. A. Vargas,
crvargas@udec.cl

Citation:
Vargas, C. A., Cuevas, L. A., Silva, N., González, H. E., De Pol-Holz, R., & Narváez, D. A. (2018). Influence of glacier melting and river discharges on the nutrient distribution and DIC recycling in the Southern Chilean Patagonia. *Journal of Geophysical Research: Biogeosciences*, *123*, 256–270. https://doi.org/10.1002/2017JG003907

Received 18 APR 2017
Accepted 20 DEC 2017
Accepted article online 28 DEC 2017
Published online 27 JAN 2018

Influence of Glacier Melting and River Discharges on the Nutrient Distribution and DIC Recycling in the Southern Chilean Patagonia

Cristian A. Vargas[1,2,3], L. Antonio Cuevas[1,2], Nelson Silva[4], Humberto E. González[5,6], Ricardo De Pol-Holz[3,7], and Diego A. Narváez[2,8]

[1]Aquatic Ecosystem Functioning Lab, Department of Aquatic System, Faculty of Environmental Sciences and Environmental Sciences Center EULA Chile, Universidad de Concepción, Concepción, Chile, [2]Center for the Study of Multiple Drivers on Marine Socio-Ecological Systems, Universidad de Concepción, Concepción, Chile, [3]Millenium Institute of Oceanography, Universidad de Concepción, Concepción, Chile, [4]Escuela de Ciencias del Mar, Pontificia Universidad Católica de Chile, Valparaíso, Chile, [5]Instituto de Ciencias Marinas y Limnológicas, Universidad Austral de Chile, Valdivia, Chile, [6]Centro de Investigación de Ecosistemas de Altas Latitudes, Universidad Austral de Chile, Valdivia, Chile, [7]GAIA-Antártica, Universidad de Magallanes, Punta Arenas, Chile, [8]Department of Oceanography and COPAS Sur-Austral, Universidad de Concepción, Concepción, Chile

Abstract The Chilean Patagonia constitutes one of the most important and extensive fjord systems worldwide, therefore can be used as a natural laboratory to elucidate the pathway of both organic and inorganic matter in the receiving environment. In this study we use data collected during an intensive oceanographic cruise along the Magellan Strait into the Almirantazgo Fjord in southern Patagonia to evaluate how different sources of dissolved inorganic carbon (DIC) and recycling may impact particulate organic carbon (POC) $\delta^{13}C$ and influence the nutrients and carbonate system spatial distribution. The carbonate system presented large spatial heterogeneity. The lowest total alkalinity and DIC were associated to freshwater dilution observed near melting glaciers. The $\delta^{13}C_{DIC}$ analysis suggests that most DIC in the upper 50 m depth was not derived from terrestrial organic matter remineralization. ^{13}C-depleted riverine and ice-melting DIC influence the DIC pool along the study area, but due to that DIC concentration from rivers and glaciers is relatively low, atmospheric carbon contribution or biological processes seem to be more relevant. Intense undersaturation of CO_2 was observed in high chlorophyll waters. Respired DIC coming from the bottom waters seems to be almost insignificant for the inorganic carbon pool and therefore do not impact significantly the stable carbon isotopic composition of dissolved organic carbon and POC in the upper 50 m depth. Considering the combined effect of cold and low alkalinity waters due to ice melting, our results highlight the importance of these processes in determining corrosive waters for $CaCO_3$ and local acidification processes associated to calving glacier in fjord ecosystems.

1. Introduction

The coastal ocean plays a key role in global biogeochemical cycles and the climatic regime on Earth. Freshwater runoff from rivers, estuaries, and fjords are recognized to influence the biogeochemistry of productive coastal areas and are important in the modification and exchange of organic and inorganic carbon between terrestrial and marine environments (Canuel, 2001).

Globally, the discharge of organic matter by rivers occurs at a rate of 20 Gt yr^{-1} (1 Gt = 1×10^{12} kg), which is similar to the accumulation rate of organic carbon in whole marine sediments (Berner & Berner, 1996; Onstad et al., 2000). This is particularly relevant during the spring season due to the increase in freshwater inputs associated to the melting of the ice accumulated during winter (Aniya, 1999). It is well known that a significant fraction of the organic matter exported by rivers and glaciers is constituted by very old material (Raymond & Bauer, 2001), unlike the new material produced in the pelagic ecosystem (Vargas et al., 2011). Chemical weathering and export of inorganic carbon from soils into rivers provide a significant amount of the atmospheric CO_2 sequestered by the terrestrial ecosystem to the coastal ocean (Cao et al., 2011). The role of freshwater input from glaciers and rivers in the biogeochemical cycles of carbon in fjord ecosystems needs necessarily to be assessed to establish the pathway of both organic and inorganic matter in the receiving environment.

The Chilean Patagonia constitutes one of the most important and extensive fjord regions worldwide, which, along with similar systems of Scandinavia, Iceland, Greenland, British Columbia, and Alaska, form some of the largest fjord areas in the world (González et al., 2013; Silva & Vargas, 2014,). This fjord system extends for over 1,600 km, which is approximately one third of the Chilean territory (Silva & Vargas, 2014). Thus, this region has a high geomorphological complexity and different hydrographic processes influence the oceanographic conditions, including, river runoff, ice melting, and oceanic intrusion. In the southern region of this large fjord system, the Strait of Magellan constitutes a major feature of the southern end of South America, connecting the Pacific Ocean with the Atlantic Ocean through a channel across the continent. This region has several features, such as (1) a complex interaction between the atmosphere, land, and the ocean (i.e., strong poleward winds and Cape Horn Current) (Strub et al., 1998), (2) enhancement of the terrigenous sediment supply (Silva et al. 2011), and (3) input of freshwater rich in terrestrial organic matter by river runoff (e.g., Bachellor river), groundwater, rainfall, and ice-melting from glaciers associated to Darwin Mountain Range that release icebergs and introduce clay/minerals and freshwater plumes into the fjord heads (Valdenegro & Silva, 2003).

Freshwater from Patagonian rivers generally contains large amount of silicic acid and organic carbon (e.g., Iriarte et al., 2007; Silva et al., 2011; Torres et al., 2011; Vargas et al., 2008), which combined with the adjacent marine nutrients support a high primary and secondary productivity in these environments (Dagg & Whitledge, 1991; Lohrenz et al., 1990). In this channel and fjord environment, the metabolic state results from a balance between primary production and respiration processes (Torres et al., 2011). Measurements of the inorganic carbon species give some insights of the biogeochemistry associated to the metabolism of this ecosystem, mainly because the recycling of inorganic carbon is related to the metabolic state through the production and uptake of CO_2 during photosynthesis and respiration (van Breugel et al., 2005). Both the pH and alkalinity also depend on the processes of remineralization of organic matter and ultimately on the ecosystem metabolism involved (Raymond & Cole, 2003).

Carbon stable isotopes ($\delta^{13}C$) have been widely used for tracing the source and fate of organic matter in aquatic ecosystems (e.g., Lafon et al., 2014; McCallister et al., 2006). In this fjord environment, the most ^{13}C-depleted dissolved organic carbon (DOC) and particulate organic carbon (POC) is oxidized/respired while sinking to deeper waters, and therefore, ^{13}C-depleted dissolved inorganic carbon (DIC) is accumulated in deep waters (van Breugel et al., 2005). When deep waters mix with the surface photic zone, it is used by plankton for both photosynthesis and calcification (e.g., cocolitophores) (van Breugel et al., 2005). Recycling of the respired CO_2 may thus result in a decrease in $\delta^{13}C$ value of organic carbon and carbonate in the fjord sediments (Schouten et al., 2000). The isotopic signature of the DIC ($\delta^{13}C_{DIC}$) is therefore a reliable measure of the carbon cycling processes in aquatic ecosystems and a powerful tool to determine how glaciers and rivers could be sources of DIC versus respired DIC escaping to surface waters and recycled in the photic zone. Furthermore, because river and glacier meltwater has low total alkalinity (A_T) and low DIC concentrations, when mixing with seawater, it decreases salinity, A_T, and DIC diminishes concentrations of CO_3^{2-} and therefore, aragonite saturation state ($\Omega_{aragonite}$) (Yamamoto-Kawai et al., 2009).

Here we report the spatial variability in the carbonate system along a transect from the western side of Magellan Strait to the Almirantazgo Fjord in southern Patagonia (Figure 1). By using information of carbonate chemistry and carbon stable isotopes we also aimed to evaluate if DIC recycling and freshwater DIC sources in the upper water column might impact the $\delta^{13}C$ pool in this stratified fjord ecosystems. With this objective we performed a study of stable carbon isotopes in different carbon pools (DIC, DOC, and POC) along this transect, including two major freshwater sources at each side of this transect, river runoff, and ice melting from calving glaciers associated to Darwin Mountain Range Ice Field. Our results are also interpreted in the context of major implications for local acidification processes in this southern Patagonia region.

2. Material and Methods

2.1. Survey Area

The study was carried out in the framework of a research cruise (*CIMAR 16 Fiordos*) conducted in the austral spring between 20 October and 12 November 2010 onboard the R/V *Abate Molina*. A single transect with 12 oceanographic sampling stations was performed from the western side of Magellan Strait (52°39′S, 74°47′W), crossing the Whiteside Channel, to the Almirantazgo Fjord (54°36.2′, 69°21′W) (Figure 1). The transect presents three deep basins (>400 m) separated by shallow constrictions-sills (Carlos III and Whiteside <100 m

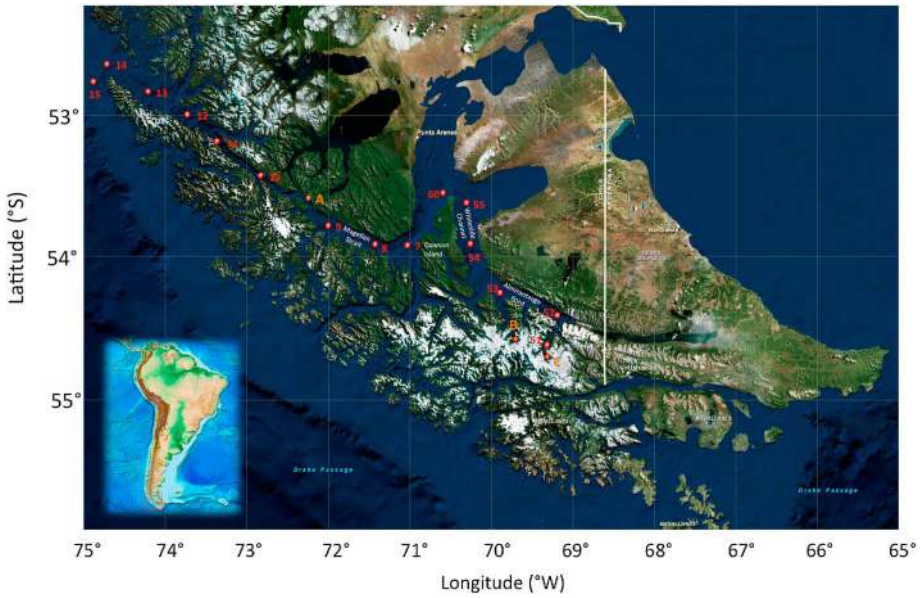

Figure 1. Study area and location of sampling stations along the Almirantazgo Fjord and Magellan Strait, for both physical and biogeochemical data. Base map from the National Center for Environmental Information, NOAA (http://maps.ngdc.noaa.gov/viewers/geophysics/). A: Bachelor River, B: Marinelli, and C: Parry Glaciers.

depth). The western basin, which is the deepest (~1,200 m depth), cover the Strait of Magellan from its western extreme coastal sill to the Carlos III Island constriction-sill. The central basin includes the central zone of the Strait of Magellan and the Whiteside Channel, whereas the south-eastern basin, includes part of the Whiteside Channel and the Almirantazgo Fjord (~200–400 m depth) and the Marinelli and Parry Glaciers, both at the head of the transect (Figure 1). The western extreme of this section connects with the Pacific Ocean and in its central part (e.g., Whiteside Channel); it is open to the Atlantic Ocean through the shallow and narrow passages called Primera and Segunda Angostura (~4.6 km wide, 50 m depth and 7.3 km wide, and 47 m depth, respectively) in the eastern side of the Strait of Magellan. In the south-eastern part of the Almirantazgo Fjord, two major calving glaciers are located, the Marinelli and Parry Glaciers, which are part of the Darwin Mountain Range Ice Field (Figure 1). This transect is also characterized by the contribution of two major freshwater sources, a small river (<20 m^3 s^{-1}), the Bachelor River (Stn A at Figure 1), which is at the western side of the transect, and the contribution due to ice melting from Marinelli and Parry Glaciers at the eastern side of the transect. (Stns B and C, respectively at Figure 1).

2.2. Sample Collection, Hydrography, Nutrients, and Chlorophyll Analyses

During the research cruise, temperature and conductivity profiles were collected with a Seabird 19 CTD, whereas water samples for different chemical analyses were collected with a Niskin bottle-rosette system. Seawater samples for dissolved oxygen and nutrient analyses were collected at discrete standard depths (1, 5, 10, 25, 75, 100, 150, 200, 250, 300, 400, 500, 600, 700, 800, and 850 m), with maximum depth of each profile determined by water depth at each station. Dissolved oxygen was determined onboard following Carpenter (1965). Apparent oxygen utilization (AOU) was estimated as the difference between the oxygen concentration at 100% saturation and the measured oxygen concentration in seawater samples. Dissolved oxygen concentration at 100% saturation was calculated following Murray and Riley (1969) using the CTD measurements of temperature and salinity.

Samples for nitrate (NO_3^-), phosphate (PO_4^{3-}), and silicic acid ($Si(OH)_4$) were kept frozen (-20°C) in 60 mL acid-cleaned high-density plastic bottles according to Gordon et al. (1994) protocol. The samples were analyzed in the Marine Biogeochemistry Laboratory of the Pontificia Universidad Católica de Valparaíso, with a nutrient auto-analyzer following Atlas et al. (1971). Water samples for chlorophyll a (Chl *a*) analyses were collected at 1, 5, 10, and 25 m depth. For Chl *a* and phaeopigments, 200 mL of seawater were filtered (MFS glass

fiber filters, 0.7 μm nominal pore size) in triplicate and immediately frozen (−20°C) until later analysis via fluorometry, using acetone (90% vol/vol) for the pigment extraction (Turner Design TD-700) according to standard procedures (Parsons et al., 1984).

Samples for DIC and DOC concentration, $\delta^{13}C_{DIC}$, $\delta^{13}C_{DOC}$, and $\delta^{18}O$, were collected at 2 and 50 m depth with a Niskin bottle-rosette system. For POC concentration and $\delta^{13}C_{POC}$ a surface sample at 2 m depth was also collected at each station. Additional surface (1 m) samples for all these analyses were also collected from a Zodiac rubber boat at the Bachelor River's mouth as well as right next to the area where ice breaks up at the Parry and Marinelli glaciers.

2.3. Estimation of the Carbonate System Parameters

Seawater samples for pH and total alkalinity (A_T) were collected at 1, 5, 10, 25, and 50 m depth. Unfortunately, samples for A_T were not collected from the Bachelor River's mouth and other potential freshwater sources. The pH samples were collected in 50 mL syringes using a Tygon tube and then transferred to a 25 mL thermostated closed cell at 25.0 ± 0.1°C for analysis with a Accumet® model 20 pH meter (input impedance $>10^{11}$ Ω, 0.1 mV sensitivity and nominal accuracy 0.001 pH units) using a glass combined single junction Ag/AgCl Metrohm electrode (code 6.0259.100). The electrode was calibrated with tris and 2-aminopyridine buffers at 25.0 ± 0.1°C (pH 8.089 and 6.786; Department of Energy (DOE), 1994), and pH values were therefore reported on the total hydrogen ion scale (Department of Energy (DOE), 1994). The estimated analysis error was estimated as <0.009 pH for most of the samples.

Samples for total A_T were stored in 500 mL borosilicate bottles, poisoned with 50 μL of saturated $HgCl_2$ solution and kept in darkness at room temperature until their analysis. A_T was determined following the Dickson et al. (2007) acid titration method. The analysis was performed with an automated titration burette (Metrohom, model Titrino Ti-Touch), in a 100 mL thermostated (25°C ± 0.5°C) closed cell (Department of Energy (DOE), 1994). The accuracy was compared to a certified reference material (supplied by Andrew Dickson, University of California, San Diego, USA) and the A_T repeatability averaged 2–3 μmol kg^{-1}. Temperature, salinity, pH_T, and A_T data were used to calculate the other parameters of the carbonate system (e.g., pCO_2 and CO_3^{2-}) and the saturation stage of Omega Aragonite ($\Omega_{aragonite}$). However, uncertainties from each measured parameters can result in uncertainties in the calculated values of carbonate system parameters, which for our estimates it would be around 6% (pCO_2) and 8% ($\Omega_{aragonite}$) (McLaughlin et al., 2015). Analyses were performed using CO2SYS software for MS Excel (Pierrot et al., 2006) with Mehrbach solubility constants (Mehrbach et al., 1973) refitted by Dickson and Millero (1987). The $KHSO_4$ equilibrium constant determined by Dickson (1990) was used for all calculations.

2.4. Dissolved Inorganic Carbon, Dissolved/Particulate Organic Carbon, and $\delta^{13}C$

For dissolved inorganic carbon (DIC) and its $\delta^{13}C$ signature, a 30 mL of seawater subsample was collected with a sterile syringe and filtered through a Swinex containing a filter of 0.2 μm and poisoned with $HgCl_2$ to halt biological activity. The septa of vials were exchanged for butyl rubber septa to prevent CO_2 diffusion. Samples were refrigerated at 5°C until their analysis (<7 days from collection). For dissolved organic carbon (DOC) and $\delta^{13}C_{DOC}$, a 30 mL subsample was collected with a sterile syringe and filtered through a Swinex containing a GF/F filter of 0.7 μm, precombusted for 4–5 h at 450°C. The samples were collected directly in 40 mL Glass 200 Series I-CHEM® vials, preventing the formation of any bubbles. Prior to analysis, DOC samples were bubbled with CO_2-free nitrogen for 7 min to ensure complete removal of dissolved inorganic carbon. For POC and $\delta^{13}C$, a surface subsample (0.5 to 2.5 L) was filtered through combusted (4–5 h at 450°C) GF/F filters to concentrate particles. Filters were dried at ~60°C for 24 h and held in a desiccator until analyzed.

All samples were run on an OI Analytical TIC-TOC Analyzer Model 1030, first run to determine the ppmC organic/inorganic concentration, then for the $\delta^{13}C$ isotope. The TIC-TOC analyzer was interfaced to a Finnigan MAT Delta Plus isotope ratio mass spectrometer for analysis by continuous flow. Data were normalized using internal standards. The analytical precision was 1.8% for the quantitative measurements and ±0.2‰ for the isotopes. Analyses were conducted in the G.G. Hatch Isotope Laboratories at the University of Ottawa, Canada.

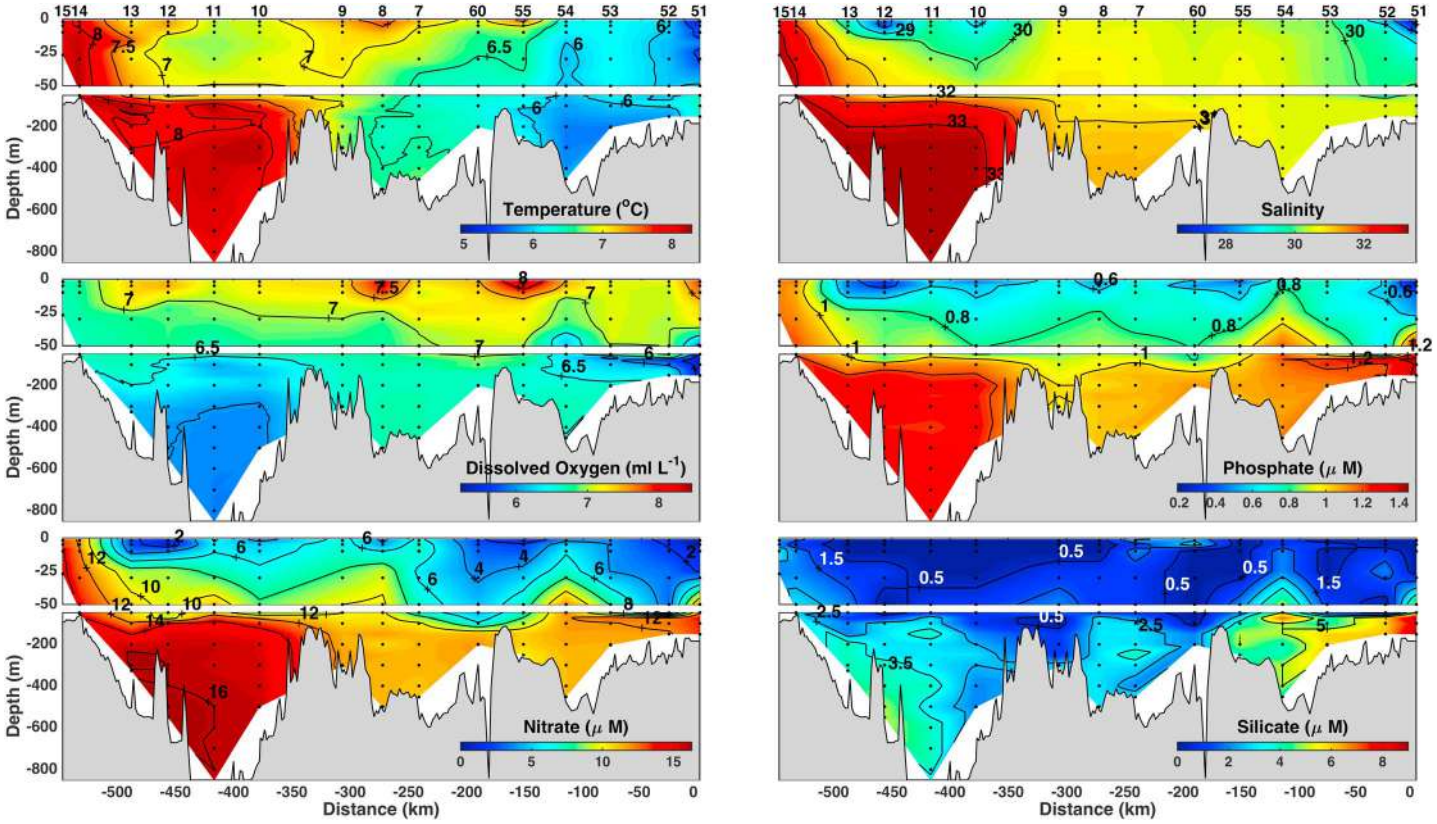

Figure 2. Vertical distribution of temperature (°C), salinity, dissolved oxygen (mL L^{-1}), phosphate (μM), nitrate (μM), and silicate (μM) from the west open of the Magellan Strait to the Marinelli and Parry Glaciers.

2.5. Oxygen Isotopes and $\delta^{18}O$

Water samples for oxygen isotopic composition were collected from seawater and ice. The $\delta^{18}O$ was analyzed by CO_2-water equilibration using 0.2 mL (fresh) or 0.6 mL (saline) of water and a gas mixture of 2% CO_2 in helium. The CO_2 was analyzed on the same Finnigan MAT Delta plus isotope ratio mass spectrometer at the G.G. Hatch Isotope Laboratories at the University of Ottawa, Canada. Although duplicates were not collected during the cruise, the analytical precision estimated from standards measured with samples was ±0.15‰. The samples were measured relative to the Vienna SMOW (VSMOW) standard, and are referenced relative to VSMOW.

3. Results

3.1. Hydrography

Large variation of the water temperature was observed along the transect, from cold waters (4–5°C) near the glaciers (Stns 51 and 52) to higher temperatures (~8°C) at the western side of the Strait of Magellan (Stns 14 and 15; Figure 2a). The vertical temperature showed a well-mixed distribution in the southeast basin near the glaciers and a weak thermocline in the central basin. A slight increase in temperature was observed between Stns 54 and 60 in the area where waters from the Almirantazgo Fjord mix with those from Magellan Strait, near Dawson Island. The western basin, below 100 m, showed an intrusion of warmer water (>7.5°C) from the Pacific Ocean (Figure 2a). A horizontal salinity gradient in the surface layer was also evidenced due to the low salinity waters (<28) close to the glaciers to high salinity (>32.0) at the western side of the Strait of Magellan (Figure 2b). The area close to Bachelor River mouth (Stn 12) also evidenced low salinity (<29 practical salinity unit (psu)) above 10 m depth (Figure 2b), giving origin to a strong halocline (~0.2 psu m^{-1}). Below 100 m a high-salinity intrusion (>33 psu) of oceanic waters sinks into the western basin (Figure 2b). Both temperature and salinity reflected the intrusion of the oceanic Pacific Sub-Antarctic Water into the western basin (Figures 2a and 2b).

3.2. Dissolved Oxygen and Nutrient Concentrations (PO_4^{3-}, NO_3^-, and $Si(OH)_4$)

Surface dissolved oxygen concentration varied largely along the transect, with higher dissolved oxygen concentration at the Whiteside Fjord (>7 mL O_2 L^{-1}, Stn 55) and lower concentration at the western side of the Magellan Strait (<7 mL O_2 L^{-1}, Stns 14 and 15) (Figure 2c). Below the well-oxygenated surface layer, dissolved oxygen tended to decrease slightly with depth to values lower than 6 mL O_2 L^{-1} below 400 m depth, mainly in the deeper western basin, and lower than 5.5 mL O_2 L^{-1} at 100 m depth at head of the Almirantazgo Fjord, hypoxic conditions (<2 mL L^{-1}; Díaz & Rosenberg, 1995; Silva & Vargas, 2014) were not observed in water column along whole the study area (Figure 2c).

Phosphate and nitrate concentrations were lower at the surface layer with minimum values (<0.5 and <2 μM, respectively) near the glaciers area and the Bachelor River outflow. Maximum values (>1 and >12 μM) were observed at the western side (Figures 2d and 2e, respectively). Below the surface layer, phosphate and nitrate concentrations increased with depth to values higher than 1.2 μM and 14 μM at 100 m depth at the Almirantazgo Fjord and below 200 m depth in the western Magellan Strait's basin (Figures 2d and 2e).

Low silicic acid concentrations were observed in the surface layer, especially in areas without the influence of the river and glacier discharges (i.e., from nondetected to 2.0 μM; Figure 2f). Below the surface layer, silicate concentration increased with depth to values higher than 6 μM at 100 m depth at the Almirantazgo Fjord. In the deep layer, silicate increased slowly to still low levels, with a maximum concentration (>4.0 μM) at 400–600 m at the western basin (Figure 2f).

3.3. Total Chlorophyll *a* (Chl *a*) and Carbonate System Variability

A patched spatial distribution was observed for surface Chl *a* (above 25 m depth) in the Almirantazgo Fjord and the Magellan Strait (Figure 3a). The lower Chl *a* concentrations were observed in low salinity ice-melting water from glaciers, whereas highest Chl *a* were observed in Stns 55, 8, and 13 in the western side of Magellan Strait.

A large spatial heterogeneity along the transect was also observed for the different carbonate system parameters estimated in our study. A nonsignificant relationship between A_T and salinity was found, which may suggest the contribution of other noncarbonate sources to A_T, and/or the possibility of more than one freshwater end-members along the study area (Figure 4a). Highest pH_T and low pCO_2 levels were associated to high Chl *a* concentration (chlorophyll > 5 μg L^{-1}) from Stns 7 to 53 along Dawson Island (Figures 3a and 3b). On the contrary, lower pH_T (<8) and higher pCO_2 (>400 μatm) levels were observed in deep waters below 25 m depth and Stn 52 at the mouth of Parry Fjord (Figures 3b and 3d). At this respect, a relationship between pCO_2 and AOU (Figure 4b) evidenced a weak but statistically significant positive correlation between both parameters ($r^2 = 0.24$, $p = 0.0001$), which although suggest that O_2 supersaturation (i.e., negative AOU levels) might be associated to autotrophic behavior (intense undersaturation of CO_2) in high Chl *a* surface waters, whereas high pCO_2 waters (>400 μatm) were associated to O_2 undersaturated (positive AOU levels) in deeper waters, mostly due to the remineralization of organic matter. This low observed correlation can be explained since low pH_T/high pCO_2 values were also observed associated to surface low salinity waters in the upper 5 m depth at Stn 52 at the Parry fjord's mouth (Figures 3b and 3d), which was also influenced by low alkalinity waters (A_T < 2,000 μmol kg sw^{-1}; Figure 3c), mostly associated to the ice-melting from Parry Glacier. Nevertheless, cold (<6°C) and low salinity waters (<28 psu) associated to this ice-melting area showed a CO_2 undersaturation in the upper 15 m depth (Figures 3d and 4b). The T-S diagram showed that waters of low salinity were characterized by well-oxygenated waters (Figure 5a), very low NO_3^- concentration due to the dilution effect of ice melting near calving glaciers (Figure 5b), and low pH (Figure 5c). Low $\Omega_{aragonite}$ ($\Omega < 1.5$) was observed in deep waters (>25 m depth) along whole transect (3F). However, almost the entire water column at Stns 51 and 52 near Parry Glacier in Almirantazgo Fjord showed $\Omega_{aragonite} < 1.5$ (Figure 3f).

3.4. Carbon Species (DIC, DOC, and POC) and Isotopic Signal

Dissolved inorganic carbon measured at surface (2 m depth) and subsurface (50 m depth) waters showed similar concentrations along the transect with values from 1,151.7 to 1,436.7 μmol kg^{-1} (Figure 6a). Freshwater samples collected at the Bachelor River mouth, and ice-glacier samples from Marinelli and Parry Glaciers evidenced a very low DIC concentration (190.8 μmol kg^{-1} and 45.8 to 116.7 μmol kg^{-1}, respectively; Figure 6a). Isotopic DIC signal ($\delta^{13}C_{DIC}$) varied from 0.7 to 1.9‰ at 2 and 50 m depth along

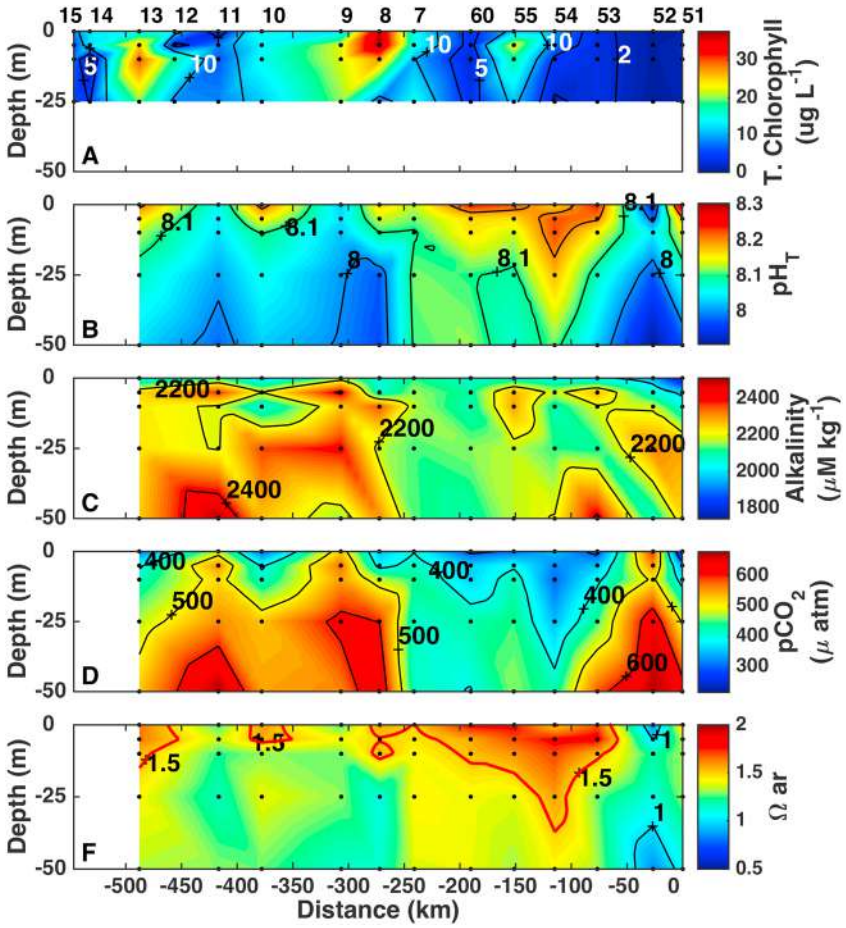

Figure 3. Vertical distribution of total chlorophyll, pH, alkalinity (μM kg^{-1} SW), pCO_2 (μatm), and $\Omega_{aragonite}$ from the west open of the Magellan Strait to the Marinelli and Parry Glaciers.

the transect (Figure 6b). Only at the west side of the Magellan Strain a single value of 0.01‰ (Stn 11) was detected at 2 m depth (Figure 6b). Depleted $\delta^{13}C_{DIC}$ values (−12.9 to −23.6‰) were detected at the Bachelor River and Marinelli and Parry Glaciers (Figure 6b). A keeling-plot of $\delta^{13}C_{DIC}$ versus 1/DIC concentration provides $\delta^{13}C$ values of respired carbon added at depth, which showed a mean $\delta^{13}C_{DIC}$ of ~3‰ (Figure 7a).

A large spatial heterogeneity in surface DOC (2 m depth) concentration was observed during our study, with highest concentration at the Almirantazgo Fjord (Stn 51) (Figure 6c). Nonsignificant differences in DOC concentration were observed between surface and subsurface (50 m depth) layers (t test = 1.289, p = 0.233). DOC concentration at the Bachelor River mouth was 1,084.2 μmol kg^{-1}, whereas ice samples from both glaciers evidenced very low DOC concentrations (Marinelli: 198.3 μmol kg^{-1}, and Parry: 81.7 μmol kg^{-1}; Figure 6c). Similar DOC isotopic signal was observed along whole transect at both surface and 50 m depth (Figure 6d). Depleted $\delta^{13}C_{DOC}$ (more than −20‰) were found at the Bachelor River and near Parry Glacier, but, in general, nonsignificant differences were found between surface and subsurface layers (t test = 1.075, p = 0.314) (Figure 6d). Surface POC also showed a large variability along the transect, with a mean range from 12,083.3 to 24,583.3 μmol kg^{-1} (Figure 6e). POC at the Bachelor River was 12,916.7 μmol kg^{-1}, whereas Marinelli Glacier showed 15,833.3 μmol kg^{-1} and Parry Glacier 9,166.7 μmol kg^{-1} (Figure 6e). Relatively constant POC isotopic signal was detected along the transect (−19.7 to −24.6‰; Figure 6f). Similar to $\delta^{13}C$-DOC the most negative values were associated to freshwater discharges (Bachelor River: −28.5‰, Marinelli Glacier: −25.2‰, and Parry Glacier: −25.8‰; Figure 6f). DOC and POC isotopic signals were positively correlated (r^2 = 0.56, p = 0.005), suggesting that most of the DOC was produced by respired POC in our study area (Figure 7b).

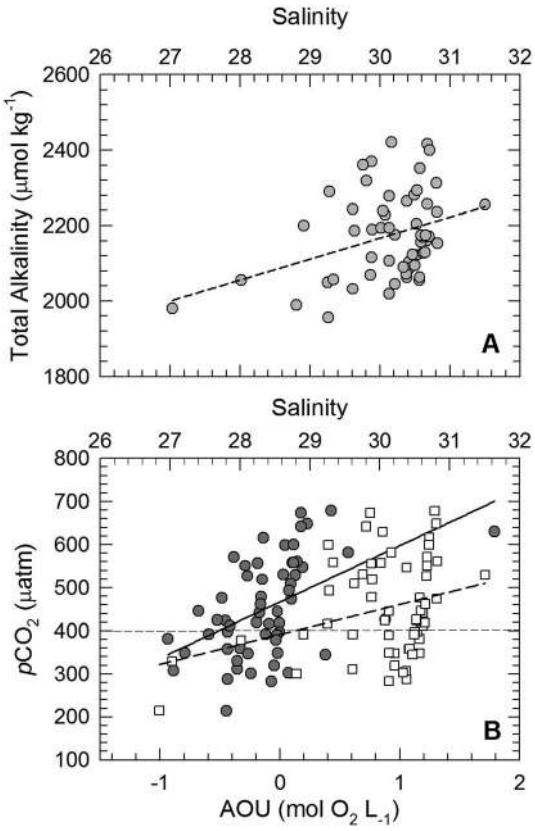

Figure 4. (a) Relationship between salinity and total alkalinity (TA = 55.55 salinity + 500.39, R^2 = 0.13, n = 57) and (b) relationship between AOU and pCO_2 (dark circles), and salinity and pCO_2 (white squares) for the study area.

3.5. Oxygen Isotopic Signal

Besides carbon isotope signals, $\delta^{18}O$ recorded at 2 and 50 m depths showed a large variability with values ranging from −0.75 to −2.35‰; Figure 8). Surface values were always more negative than at 50 m depth mainly near the glacier area. The oxygen isotopic signal showed strong negative values associated to the freshwater discharges from the Bachelor River and from the ice-melting water at both glaciers (Figure 8). This trend is also observed under the salinity gradient, where the Parry Glacier ice water $\delta^{18}O$ values was −5.4‰ while −12.6‰ in Marinelli Glacier ice and −10.8‰ in ice-melting derived freshwater carried by the Bachellor river (Figures 8 and 9).

4. Discussion

4.1. Physical-Chemical Spatial Variability

The hydrography conditions were dominated by the intrusion of Sub-Antarctic waters (SAAW) from the Pacific Ocean in the western Magellan Strait below 150 m deep and Estuarine Waters (EW) in the surface layer (0–100 m) and eastern side of the study area (Palma & Silva, 2004). Due to its higher density, the warmer, saltier, and nutrient-rich SAAW sink into the Magellan Strait western basin, filling it and reaching distances of ~200 km toward the strait's inner part. The surface layer receives cold freshwater discharges mainly from the Bachelor River and the Marinelli and Parry Glaciers, and runoff inputs from the Darwin Mountain Range, originating the EW. The T-S diagrams showed that EW was not only characterized by low salinity and high oxygen, but also by low NO_3^-/pH conditions. The mixing of SAAW with EW forms the modified Sub-Antarctic Water in the intermediate part of the study area (Palma & Silva, 2004). The intrusion of denser water in the west initiates an estuarine-like circulation with deep SAAW flowing eastward and surface EW flowing westward. However, the shallow Carlos III constriction-sill (50–100 m deep) in the western Magellan Strait inhibits the circulation, increasing the retention time in the surface and subsurface layer at both sides of the sill.

Low nutrient concentrations prevailed in the study area. Phytoplankton consumption and freshwater from rivers, runoff, glaciers melting, and rainfall can have low nutrient content (Panella et al., 1991; Silva & Vargas, 2014). High nitrate (~16 μM) and phosphate (>1.2 μM) values were observed below 200 m at the western side of the Magellan Strait influenced by the inflow of SAAW. Surface nitrate and phosphate values were lower than previously reported (e.g., Iriarte et al., 2001; Torres et al., 2011; Valdenegro & Silva, 2003). The low nutrient concentrations can be due to the presence of a shallow sill (<100 m depth) in the western basin, which can reduce the injection of waters rich in nitrate and phosphate to the surface layer or increase the residence time of the surface water increasing the consumption time of nutrients, as well as biological consumption by phytoplankton. In this sense, high Chl *a* values suggest an important uptake by phytoplankton. Silicic acid concentrations were low for the entire study area compared to other channels in Patagonia. The rivers that flow into the fjords of northern Patagonia (~41.5–46.5°S) typically transport high silicic acid concentrations (20–100 μM; Silva, 2008). In the study area, there is only one small river (Bachelor River <20 $m^3\ s^{-1}$, Stn 12), and it has been suggested that lower total DSi can be expected below 51°S due to reduced runoff and potential small load of silicic acid surface layers (Torres et al., 2014). However, there is also the possibility that the contribution of silicic acid can be almost immediately utilized for phytoplankton growth resulting in Si limitation in the region. The weathering and loading of bioavailable silicic acid is a result of lithology, vegetation cover, precipitation, and temperature (Conley et al., 2006). The steep slopes in the coastal zone of the studied area, small watersheds giving origin to short and low river's flows (<1 $m^3\ s^{-1}$), runoff, limited soil, and poor development of vascular plants seems to reduce the silicic acid levels of the freshwater being discharged into the surface waters (Torres et al., 2011). Silicic acid values of 8 μM near the glacier area and below

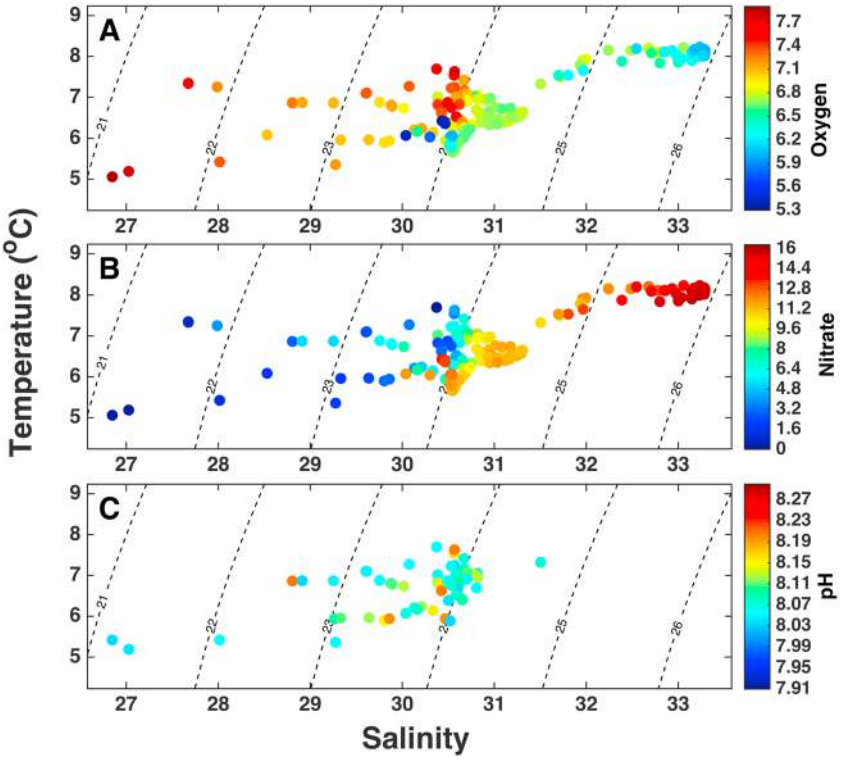

Figure 5. Temperature/salinity (TS) diagram for the data collected in the study area. The colors in the TS diagrams represent (a) dissolved oxygen (mL L^{-1}), (b) nitrate (μM), and (c) pH. Data are shown in Figure 2 (dissolved oxygen and nitrate) and Figure 3 (pH).

200 m depth may be due to glacier erosion (Anderson, 2006) keeping low values at surface due to phytoplankton uptake, and due to remineralization in deep layers (Silva & Vargas, 2014).

Phytoplankton biomass may be supported mainly by the available nutrients and light in fjords of the Chilean Patagonia (Iriarte et al., 2013; Jacob et al., 2014). In this case, the available nitrate and phosphate originated mainly from SAAW (<200 m) were probably used by the existing phytoplankton biomass, keeping it higher than 10 μg L^{-1} in some sites above the surface layer. Compared to previous reports in the same area and period (Iriarte et al., 2001) Chl *a* values were five times higher during this study. Additionally, the phytoplankton biomass estimated consisted of cells larger than 20 μm (data not showed), which is consistent with spring phytoplankton bloom and rapid nitrate uptake. A simple $Si(OH)_4/NO_3$ calculation shows that the average ratio is usually <1, leading to a partial silicic acid limitation for diatom growth (Turner et al. 1988). Thus, the phytoplankton biomass in the study area was a mixture of dinoflagellates and chain-forming diatoms, such as the genera *Pseudo-nitschia*, *Thalassiosira*, and *Chaetoceros* (González et al., 2016).

4.2. Carbonate System and Sources of Inorganic and Organic Carbon in the Study Area

Quantifying the processes controlling dissolved inorganic carbon (DIC) dynamic in aquatic ecosystems is essential for estimations of the ecosystem carbon budget. The inorganic geochemical processes occurring in Sub-Antarctic fjord and channels influenced by freshwater discharges from both river and ice melting are still poorly understood. Our results evidenced that carbonate system along Almirantazgo Fjord and Magellan Strait showed a large spatial heterogeneity. The lowest A_T and DIC were associated to freshwater dilution observed at the stations near the Perry and Marinelli glaciers. Similar results have been found in other Artic tidewater-glacier fjord (Fransson et al., 2015) and in Antarctic surface waters near outflowing glaciers (Mattsdotter Björk et al., 2014). The values of DIC and pCO_2 were in the mean range for a high-latitude fjord ecosystem (Fransson et al., 2015; Torres et al., 2011). Below 25 m depth, the water has higher pCO_2 (>500 μatm) and relatively lower pH (<8.1) than in surface oxygenated waters.

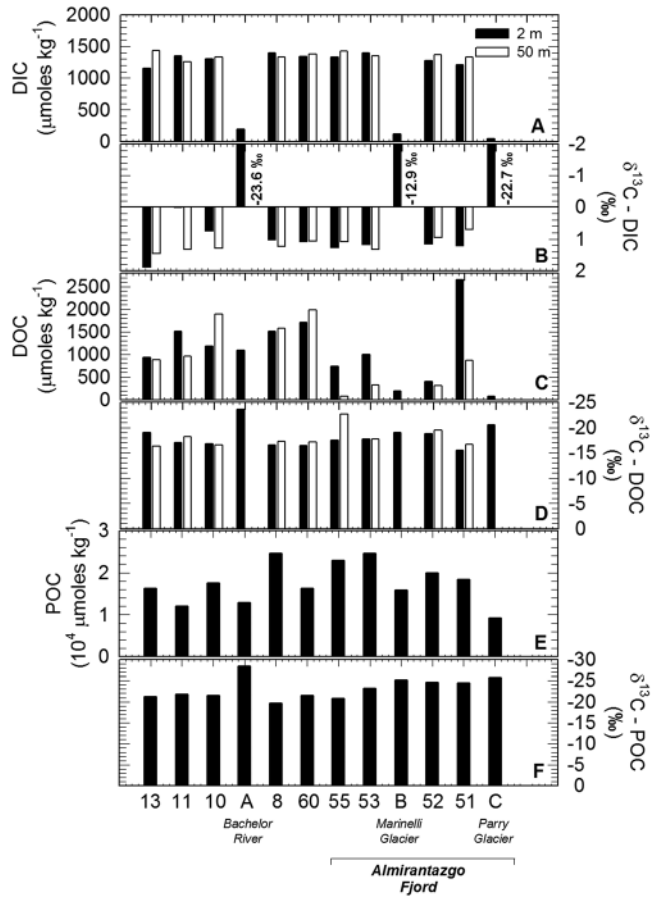

Figure 6. (a) Dissolved inorganic carbon, (b) ^{13}C-DIC, (c) dissolved organic carbon, (d) ^{13}C–DOC, (e) particulate organic carbon, and (f) ^{13}C-POC, from the west open of the Magellan Strait to the Marinelli and Parry Glaciers at 2 and 50 m depth.

The linear regression of measured $\delta^{13}C_{DIC}$ versus 1/DIC showed a *y* intercept of ~3‰ (Figure 7a), which suggests that most DIC in the upper 50 m was not originated from organic matter remineralization. In fact, we did not observe significant differences in $\delta^{13}C_{DIC}$ between surface and subsurface layer at 50 m depth (Figure 6b). We do not know if in deeper waters we could observe a more significant contribution of respired CO_2 to DIC pool (as observed in some Norwegian Fjord; van Breugel et al., 2005); however, at least during this austral spring, respired DIC coming from the bottom waters seems to be almost insignificant for the inorganic carbon pool in the upper 50 m. Moreover, this area along the Almirantazgo Fjord and Magellan Strait is characterized by well-oxygenated waters (i.e., >6 mL O_2 L^{-1}) from surface to bottom (1,200 m maximum depth; Figure 2c). In addition, ^{13}C-depleted riverine and ice-melting DIC, clearly derived from terrestrial organic matter respiration, did not influenced the DIC pool along the study area, since DIC concentration in both freshwater sources was extremely low (<200 μmol kg^{-1}) and large river discharges are not observed in this region. In consequence, $\delta^{13}C_{DIC}$ values suggest that DIC available for photosynthesis is almost completely derived from atmospheric CO_2 dissolution, which indeed showed pCO_2 values <400 μatm in the surface layer, suggesting an intense undersaturation of CO_2 (i.e., from Stn 7 to Stn 53; Figure 3), with the exception of a strong gradient along Parry Fjord, with pCO_2 oversaturation at the fjord's mouth (Figure 3). Similar CO_2 gradient have been observed during the austral spring along the Ballena Fjord within the Magellan Strait, from low pCO_2 at the head of the fjord, close to the glacier, to higher levels at the fjord's mouth (Torres et al., 2011). The fjord and inner channels in Southern Patagonia are typically characterized by stratified conditions (González et al., 2013; Valdenegro & Silva, 2003), and this stratified condition occasionally acts as a sink for CO_2 (Torres et al., 2011). Moreover, the rapid depletion of DIC in high chlorophyll surface waters results in a significant atmospheric CO_2 uptake in the upper surface layers, as evidenced by the isotopic signature of DIC during our research cruise (i.e., $\delta^{13}C_{DIC}$ 1–2‰). In consequence, respired carbon should not impact significantly the stable carbon isotopic composition of the DOC and POC pools. Indeed, $\delta^{13}C_{DOC}$ did not showed a significant heterogeneity and it ranged from −18 and −20‰. The relationship between $\delta^{13}C_{DOC}$ and $\delta^{13}C_{POC}$ suggests that in some proportion, POC constituted a significant source to the DOC pool in the study area. However, DOC concentration was very high in the western side of the Magellan Strait (>1,000 μmol kg^{-1}) and maximum at the head of the Parry Fjord (>2,500 μmol kg^{-1}). Similarly, POC concentration was relatively high in this area, despite the very low chlorophyll concentration (<2 μg L^{-1}; Figure 3a). In consequence, it can also suggests that the possibility that POC in the ice-melting influenced area can be eolian and/or captured by glaciers or petrogenic and sourced from bedrock erosion in the Parry Glacier. It is well known that sedimentary organic carbon in fjords is largely composed of three components, marine biospheric, terrestrial biospheric, and petrogenic organic carbon (Smith et al., 2015). Considering our $\delta^{13}C_{DOC}$ values, the high DOC concentration observed, did not seem to be only associated to phytoplankton-derived POC respiration, but also rapid breakdown of petrogenic POC as evidenced for other glacier-influenced fjord areas (Cui et al., 2016, 2017). Recycling of petrogenic organic carbon is of significant importance in the global carbon cycle since its oxidation represents a substantial carbon source to the atmosphere, whereas the fraction escaping to oxidation can be reburied in marine sediments having minimal effect in the modern carbon cycle (Galy et al., 2015).

The $\delta^{13}C_{POC}$ values found during our study suggest autotrophic production by marine phytoplankton, which typically range between −18‰ and −24‰ (Tyson, 1995), as a consequence of isotopic fractionation during DIC uptake by photosynthesis (Hayes, 2001). Indeed, the photoautotrophic carbon isotope fractionation between DIC and POC, ε_p can be calculated using the equation suggested by van Breugel et al., 2005. The

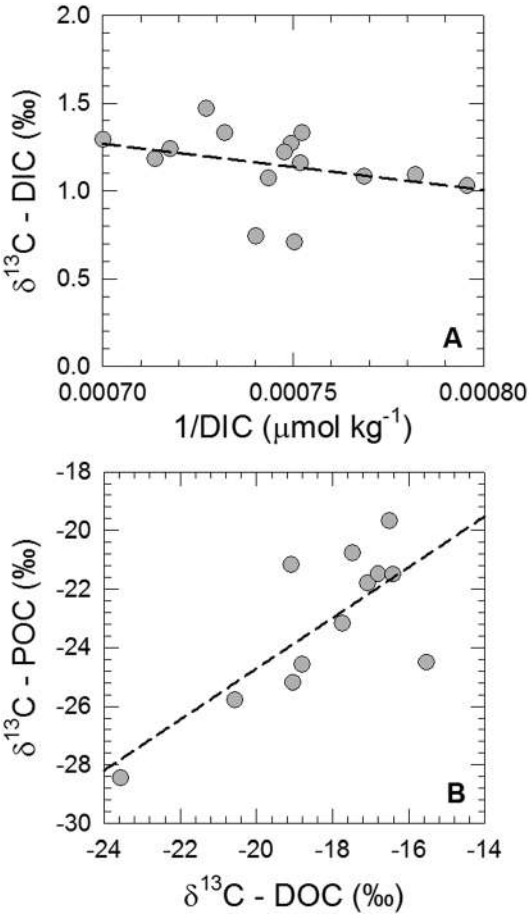

Figure 7. Relationship between (a) δ^{13}C-DIC (‰)versus 1/DIC and (b) δ^{13}C-POC versus δ^{13}C-DOC (‰) in the study area.

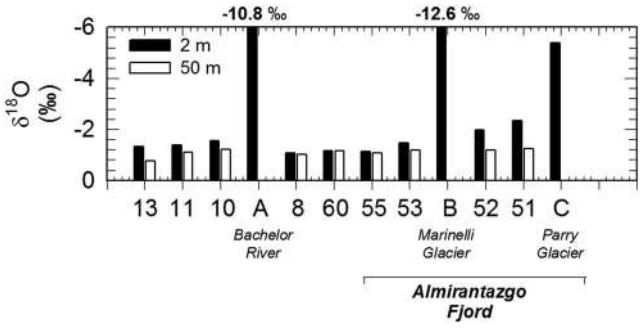

Figure 8. δ^{18}O (‰) from the west open of the Magellan Strait to the Marinelli and Parry Glaciers at 2 and 50 m depth.

estimated ε_p ranged from 21.3 to 26.3‰ in surface waters, which is in the range for the maximum fractionation associated with Rubisco for marine photosynthetic algae (~25‰; Hayes, 2001).

Oxygen isotopic analyses have also evidenced that there is a single water mass spanning from the surface to at least 50 m depth all along the transect. The δ^{18}O analysis in the meltwater from Marinelli and Parry Ice showed large differences that point out to perhaps new ice being formed from a mixture of rain and seawater near the Parry during winter. Finally, the δ^{18}O isotopic results showed little freshwater influence along the transect, except at stations very close to a freshwater input like the Bachellor River (Figure 9).

4.3. Influence of Ice Melting on Ocean Acidification State

Sub-Antarctic fjord ecosystems could be particularly vulnerable to ocean acidification due to the cold and relatively fresh surface waters, which have great potential for CO_2 uptake. However, there are almost no observations of the natural spatial variability of the carbonate system in this region, and particularly at our knowledge, this is the first detailed study of the carbonate system in a high-latitude fjord system (Almirantazgo Fjord-Magellan Strait region in Patagonia).

Different processes might affect the $CaCO_3$ saturation state (Ω) in this region, such as air-ocean CO_2 exchange; biological processes, such as photosynthesis and respiration; and physical processes such as temperature and salinity changes, river discharges, and glacier melt. Similar to what we have found for the ice-melting waters at the Parry Fjord, different studies have shown that sea ice meltwater result in low Ω due to dilution of A_T and CO_3^{2-} concentration in cold waters of high-latitude fjord ecosystems (Chierici & Fransson, 2009; Evans et al., 2014; Yamamoto-Kawai et al., 2009), which in turns gives a positive feedback on ocean acidification by decreasing the pH. Therefore, increasing ice melting could be a significant challenge for calcifying pelagic and benthic organisms inhabiting the Southern Patagonia, such as pelagic pteropods (Roberts et al., 2011), echinoderms (Arntz et al., 1994), and gastropods (Newcombe & Cárdenas, 2011). This area holds important benthonic fisheries like king crab, mussel, and sea urchin, all of which could be affected by decreasing pH. Moreover, although $CaCO_3$ subsaturation ($\Omega < 1$) was only observed at Stn 52 at the Parry Fjord's mouth, $\Omega < 1.5$ were observed almost through all the studied area, with the exception of the central part near Dawson Island (Stns 60, 55, and 54). At this respect, it is well known that some marine calcifiers, such as, bivalves require Ω values higher than 1.6 during larval stages to adequately incorporate $CaCO_3$ (Barton et al., 2012; Salisbury et al., 2008). The regional implications could be very complex depending on climate and intrinsic glacier dynamics affecting the coastal ocean. For example, the western side of Patagonia has been characterized by high freshwater discharge and melting ice (Dávila et al., 2002). In that respect, Rignot et al. (2003) demonstrated that glaciers in Patagonia are thinning more quickly than can be explained by global warming and decreased precipitation, and even their contribution to sea level per unit area can be larger than that from Alaska glaciers. Accordingly, we hypothesize that ice melting in calving glaciers in some locations of Patagonia could impact substantially marine calcifiers populations. However, the spatial extents of this physiological threshold as well as the implications on carbon cycling are relatively unknown, and more data are needed to test these ideas.

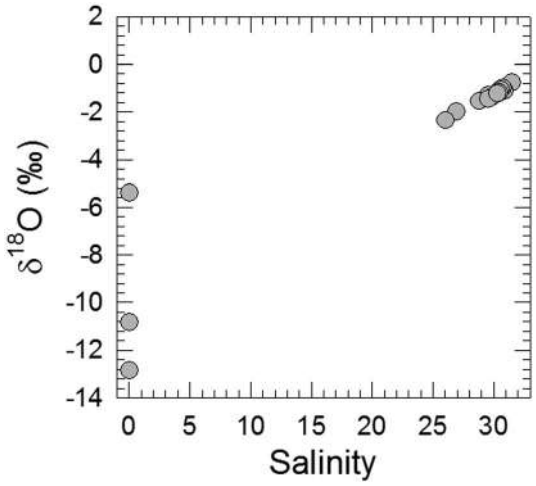

Figure 9. Relationship between $\delta^{18}O$ (‰) and salinity (psu) for freshwater samples (riverine freshwater and ice samples) and samples collected along the Magallanes-Almirantazgo transect.

The highest pH, low pCO_2, and high Ω observed near the Dawson Island and Whiteside Channel coincided with relatively high Chl *a* concentration. Indeed, strong thermal/salinity gradients as observed in this area are known to induce primary production due to upwelling of nutrient and mineral-rich water as a result of glacial plumes (e.g., Lydersen et al., 2014). Indeed, González et al. (2016) have also reported a high productivity associated to this region, and it is well known that biological production consumes DIC, and therefore result in an increase in pH and Ω.

Considering that most of processes determining Ω can be affected under climate change scenarios, the combined effect of cold and relatively low alkalinity waters due to ice melting, our results highlight the importance of these processes in determines corrosive waters for $CaCO_3$ and local acidification processes associated to calving glacier in fjord ecosystems. In consequence, our results evidence the importance of future studies dealing with the spatial-temporal variability of ice-melting waters in Sub-Artic and Sub-Antartic fjord regions affected by warming and/or glacier retreat, in order to understand the vulnerability for marine calcifying organisms to the changing ocean.

5. Conclusions

In this study we addressed how different sources of DIC (mostly riverine discharges and glacier melting) and recycling may impact POC $\delta^{13}C$ and influence nutrients and carbonate system spatial distribution along a Sub-Antarctic fjord channel system in the southern Chilean Patagonia.

The observed low nutrient concentration might be a consequence of the combined effects of a diminished nutrient supply to the surface due to the presence of a shallow sill, which reduces the injection of high nutrient SAAW with biological consumption by phytoplankton.

The carbonate system showed a large spatial and temporal heterogeneity. The lowest A_T and DIC were associated to freshwater dilution observed near melting glaciers. The $\delta^{13}C_{DIC}$ analysis suggests that most DIC in the upper 50 m depth was not derived from organic matter remineralization. ^{13}C-depleted riverine and ice-melting DIC that seem do not influence the DIC pool along the study area, mostly due to DIC concentration from freshwater sources (rivers and glaciers), are relatively insignificant. Intense undersaturation of CO_2 was observed in high chlorophyll waters. Respired DIC coming from the bottom waters seems to be almost insignificant for the inorganic carbon pool and therefore do not impact significantly the stable carbon isotopic composition of DOC and POC in the upper 50 m depth.

Although $CaCO_3$ subsaturation ($\Omega < 1$) was only observed at the Parry Fjord's mouth, $\Omega < 1.5$ were observed almost through all the studied area, with the exception of an area near Dawson Island. Considering the

combined effect of cold and relatively low alkalinity water due to ice melting, our results highlight the importance of these processes in determining corrosive waters for $CaCO_3$ and local acidification processes associated to calving glacier in fjord ecosystems of Chilean Patagonia.

Acknowledgments

This work was supported by the projects CONA C16F 09-15 (granted to C. Vargas), CONA C16F 09-08 (granted to N. Silva), CONA C16F 09-10 (granted to H.E. González), and Fondecyt 1130254 by CONICYT. Additional support from the Millennium Nucleus *"Center for the Study of Multiple-drivers on Marine Socio-Ecological Systems (MUSELS)"* funded by MINECON NC120086 and the *Millennium Institute of Oceanography (IMO)* funded by MINECON IC120019 is also acknowledged. R.D.P.-H. acknowledges support from FONDAP 15110009. H. E. G. also acknowledges additional support from FONDAP 15150003. The authors would like to thank to E.K. Cascales for their valuable help and support during sampling and laboratory analysis and to P. Reinoso for the dissolved oxygen, nutrient, pH, and total alkalinity sampling and chemical analysis. C.A.V. is supported by Red Doctoral REDOC.CTA, MINEDUC project UCO1202 at U. de Concepción. Data are included as a table as supporting information in an Adobe Acrobat file; any additional data may be obtained by sending a written request to the corresponding authors (Cristian A. Vargas; e-mail: crvargas@udec.cl).

References

Anderson, S. (2006). Impact of mineral surface area on solute fluxes at Bench Glacier, Alaska. In P. G. Knight (Ed.), *Glacier science and environmental change* (pp. 75–78). London: Blackwell. https://doi.org/10.1002/9780470750636.ch16

Aniya, M. (1999). Recent glacier variations of the Hielos Patagónicos, South America and their contribution to sea-level change. *Arctic, Antarctic, and Alpine Research*, *31*(2), 165–173. https://doi.org/10.2307/1552604

Arntz, W. E., Brey, T., & Gallardo, A. (1994). Antarctic zoobenthos. *Oceanography and Marine Biology*, *32*, 241–304.

Atlas, E. S., Hager, S., Gordon, L., & Park, P. (1971). A practical manual for use of the Technicon Autoanalyser in sea water nutrient analyses (Technical Report). Oregon State University, Department of Oceanography.

Barton, A., Hales, B., Waldbusser, G. G., Langdon, C., & Feely, R. A. (2012). The Pacific oyster, Crassostrea gigas, shows negative correlation to naturally elevated carbon dioxide levels: Implications for near-term ocean acidification effects. *Limnology and Oceanography*, *57*(3), 698–710. https://doi.org/10.4319/lo.2012.57.3.0698

Berner, E. K., & Berner, R. A. (1996). *Global environment: Water, air, and geochemical cycles* (p. 376). New Jersey: Prentice Hall.

Canuel, E. A. (2001). Relations between river flow, primary production and fatty acid composition of particulate organic matter in San Francisco and Chesapeake Bays: A multivariate approach. *Organic Geochemistry*, *32*(4), 563–583. https://doi.org/10.1016/S0146-6380(00)00195-9

Cao, L., Bala, G., & Caldeira, K. (2011). Why is there a short-term increase in global precipitation in response to diminished CO_2 forcing? *Geophysical Research Letters*, *38*, L06703. https://doi.org/10.1029/2011GL046713

Chierici, M., & Fransson, A. (2009). Calcium carbonate saturation in the surface water of the Arctic Ocean: Undersaturation in freshwater influenced shelves. *Biogeosciences*, *6*, 2412–2431.

Conley, D. J., Sommer, M., Meunier, J. D., Kaczorek, D., & Saccone, L. (2006). Silicone in the terrestrial biosphere. In V. Ittekot, D. Unger, C. Humborg, & N. T. An (Eds.), *The silicon cycle: Human perturbations and impact on aquatic systems* (Chap. 3, pp. 13–28). Washington, DC: Island Press.

Cui, X., Bianchi, T. S., Hutchings, J. A., Savage, C., & Curtis, J. H. (2016). Partitioning of organic carbon among density fractions in surface sediments of Fiordland, New Zealand. *Journal of Geophysical Research: Biogeosciences*, *121*, 1016–1031. https://doi.org/10.1002/2015JG003225

Cui, X., Bianchi, T. S., & Savage, C. (2017). Erosion of modern terrestrial organic matter as a major component of sediments in fjords. *Geophysical Research Letters*, *44*(3), 1457–1465. https://doi.org/10.1002/2016GL072260

Dagg, M. J., & Whitledge, T. E. (1991). Concentrations of copepod nauplii in the nutrient-rich plume of the Mississippi River. *Continental Shelf Research*, *11*(11), 1409–1423. https://doi.org/10.1016/0278-4343(91)90043-6

Dávila, P. M., Figueroa, D., & Müller, E. (2002). Freshwater input into the coastal ocean and its relation with the salinity distribution off austral Chile (35–55°S). *Continental Shelf Research*, *22*, 521–534. https://doi.org/10.1016/S0278-4343(01)00072-3

Department of Energy (DOE) (1994). In A. G. Dickson & C. Goyet (Eds.), *Handbook of methods for the analysis of the various parameters of the carbon dioxide system in seawater*. Santiago: ORNL/CDIAC-74.

Díaz, R. J., & Rosenberg, R. (1995). Marine benthic hypoxia: A review of its ecologicaleffects and the behavioral responses of benthic macrofauna. *Oceanography and Marine Biology*, *33*, 245–303.

Dickson, A. G. (1990). Standard potential of the reaction: AgCl(s) + $1.2H_2$(g) = Ag(s) + HCl (aq), and the standard acidity constant of the ion HSO^{-}_{4} in synthetic sea water from 273.15 to 318.15. *The Journal of Chemical Thermodynamics*, *22*(2), 113–127. https://doi.org/10.1016/0021-9614(90)90074-Z

Dickson, A. G., & Millero, F. J. (1987). A comparison of the equilibrium constants for the dissociation of carbonic acid in seawater media. *Deep Sea Research Part A*, *34*(10), 1733–1743. https://doi.org/10.1016/0198-0149(87)90021-5

Dickson, A. G., Sabine, C. L., & Christian, J. R. (2007). *Guide to best practices for ocean CO_2 measurements. PICES Special Publication* (p. 173). Sidney, British Columbia: North Pacific Marine Science Organization (PICES).

Evans, W., Mathis, J. T., & Cross, J. N. (2014). Calcium carbonate corrosivity in an Alaskan inland sea. *Biogeosciences*, *11*, 365–379. https://doi.org/10.5194/bg-11-365-2014

Fransson, A., Chierici, M., Nomura, D., Granskog, M. A., Kristiansen, S., Martma, T., & Nehrke, G. (2015). Effect of glacial drainage water on the CO_2 system and ocean acidification state in an Arctic tidewater-glacier fjord during two contrasting years. *Journal of Geophysical Research: Oceans*, *120*, 2413–2429. https://doi.org/10.1002/2014JC010320

Galy, V., Peucker-Ehrenbrink, B., & Eglinton, T. (2015). Global carbon export from the terrestrial biosphere controlled by erosion. *Nature*, *521*(7551), 204–207. https://doi.org/10.1038/nature14400

González, H. E., Castro, L., Daneri, G., Iriarte, J. L., Silva, N., Tapia, F., … Vargas, C. A. (2013). Land–ocean gradient in haline stratification and its effects on plankton dynamics and trophic carbon fluxes in Chilean Patagonian fjords (47–50°S). *Progress in Oceanography*, *119*, 32–47. https://doi.org/10.1016/j.pocean.2013.06.003

González, H. E., Graeve, M., Kattner, G., Silva, N., Iriarte, J. L., Osmán, L., … Vargas, C. A. (2016). Carbon flow through the pelagic food web in southern Chilean Patagonia: Relevance of *Euphausia vallentini* as a key species. *Marine Ecology Progress Series*, *557*, 91–110. https://doi.org/10.3354/meps11826

Gordon, L. I., Jennings, J. C., Ross, A. A., & Krest, J. M. (1994). WOCE operation manual. Section 2. A suggested protocol for continuous flow automated analysis of seawater nutrients (pp. 1–52).

Hayes, J. (2001). Fractionation of the isotopes of carbon and hydrogen in biosynthetic processes. In J. W. Valley & D. R. Cole (Eds.), *Stable isotopic geochemistry*, *Reviews in Mineralogy* (Vol. 43, pp. 225–278). Washington, DC: Mineralogical Society of America.

Iriarte, J. L., Kush, A., Osses, J., & Ruiz, M. (2001). Phytoplankton biomass in the sub-Antarctic area of Straits of Magellan (53°S), Chile during spring-summer 1997/1998. *Polar Biology*, *24*(3), 154–162. https://doi.org/10.1007/s003000000189

Iriarte, J. L., González, H. E., Liu, K. K., Rivas, C., & Valenzuela, C. (2007). Spatial and temporal variability of chlorophyll and primary productivity in surface waters of southern Chile (41.5–43°S). *Estuarine, Coastal and Shelf Science*, *74*(3), 471–480. https://doi.org/10.1016/j.ecss.2007.05.015

Iriarte, J. L., Pantoja, S., González, H. E., Silva, G., Paves, H., Labbé, P., … Häussermann, V. (2013). Assessing the micro-phytoplankton response to nitrate in Cumao Fjord (42°S) in Patagonia (Chile), using a microcosm approach. *Environmental Monitoring and Assessment*, *185*(6), 5055–5070. https://doi.org/10.1007/s10661-012-2925-1

Jacob, B., Tapia, F. J., Daneri, G., Iriarte, J. I., Montero, P., Sobarzo, M., & Quiñones, R. A. (2014). Springtime size-fractionated primary prodution across hydrographic and PAR-light gradients in Chilean Patagonia (41–50°S). *Progress in Oceanography*, *129*, 75–84. https://doi.org/10.1016/j.pocean.2014.08.003

Lafon, A., Silva, N., & Vargas, C. A. (2014). Contribution of allochthonous organic carbon across the Serrano River Basin and the adjacent fjord system in Southern Chilean Patagonia: Insights from the combined use of stable isotope and fatty acid biomarkers. *Progress in Oceanography*, *129*, 98–113. https://doi.org/10.1016/j.pocean.2014.03.004

Lohrenz, S. E., Dagg, M. J., & Whitledge, T. E. (1990). Enhance primary production at the plume/oceanic interfase of the Mississippi River. *Continental Shelf Research*, *10*(7), 639–664. https://doi.org/10.1016/0278-4343(90)90043-L

Lydersen, C., Assmy, P., Falk-Petersen, S., Kohler, J., Kovacs, K. M., Reigstad, M., … Zajaczkowski, M. (2014). The importance of tidewater glaciers for marine mammals and seabirds in Svalbard, Norway. *Journal of Marine Systems*, *129*, 452–471. https://doi.org/10.1016/j.jmarsys.2013.09.006

Mattsdotter Björk, M., Fransson, A., Torstensson, A., & Chierici, M. (2014). Ocean acidification state in western Antarctic surface waters: Controls and interannual variability. *Biogeosciences*, *11*(1), 57–73. https://doi.org/10.5194/bg-11-57-2014

McCallister, S. L., Bauer, J. E., Ducklow, H. W., & Canuel, E. A. (2006). Sources of estuarine dissolved and particulate organic matter: A multi-tracer approach. *Organic Geochemistry*, *37*(4), 454–468. https://doi.org/10.1016/j.orggeochem.2005.12.005

McLaughlin, K., Weisberg, S. B., Dickson, A., Hofmann, G. E., Newton, J. A., Aseltine-Neilson, D., … Steele, B. (2015). Core principles of the California Current Acidification Network: Linking chemistry, physics, and ecological effects. *Oceanography*, *25*(2), 160–169. https://doi.org/10.5670/oceanog.2015.39

Mehrbach, C., Culberson, C. H., Hawley, J. E., & Pytkowicz, R. M. (1973). Measurement of the apparent dissociation constants of carbonic acid in seawater at atmospheric pressure. *Limnology and Oceanography*, *18*(6), 897–907. https://doi.org/10.4319/lo.1973.18.6.0897

Murray, C. N., & Riley, J. P. (1969). The solubility of gases in distilled water and seawater. 2. Oxygen. *Deep Sea Research*, *16*, 311–320.

Newcombe, E. M., & Cárdenas, C. A. (2011). Rocky reef benthic assemblages in the Magellan Strait and the South Shetland Islands (Antarctica). *Revista de Biología Marina y Oceanografía*, *46*(2), 177–188. https://doi.org/10.4067/S0718-19572011000200007

Onstad, G. D., Canfield, D. E., Quay, P. D., & Hedges, J. I. (2000). Sources of particulate organic matter in rivers from the continental USA:Lignin phenol and stable carbon isotope compositions. *Geochimica et Cosmochimica Acta*, *64*(20), 3359–3546.

Palma, S., & Silva, N. (2004). Distribution of siphonophores, chaetognaths, euphausiids and oceanographic conditions in the fjords and channels of southern Chile. *Deep Sea Research Part II: Topical Studies in Oceanography*, *51*(6-9), 513–535. https://doi.org/10.1016/j.dsr2.2004.05.001

Panella, S., Michellato, A., Perdicaro, R., Magazzu, G., Decembrini, F., & Scarazzato, P. (1991). A preliminary contribution to understanding the hidrological characteristics of the strain of Magellan: Austral spring 1989. *Bollettino Oceanology Teorica ed Applicata*, *9*(2–3), 107–126.

Parsons, T. R., Maita, Y., & Lalli, C. M. (1984). *A manual of chemical and biological methods for seawater analysis* (173 pp.). Oxford: Pergamon Press.

Pierrot, D., Lewis, E., & Wallace, D. W. R. (2006). MS Excel program develop for CO_2 system calculations, ORNL/CDIAC-105. Carbon dioxide information analysis center. Oak Ridge, TN: Oak Ridge National Laboratory, U.S. Department of Energy.

Raymond, P. A., & Bauer, J. E. (2001). Riverine export of aged terrestrial organic matter to the North Atlantic Ocean. *Nature*, *409*(6819), 497–500. https://doi.org/10.1038/35054034

Raymond, P. A., & Cole, J. J. (2003). Increase in the export of alkalinity from North America's Largest River. *Science*, *301*(5629), 88–91. https://doi.org/10.1126/science.1083788

Rignot, E., Rivera, A., & Casassa, G. (2003). Contribution of the Patagonia Icefields of South America to sea level rise. *Science*, *302*(5644), 434–437. https://doi.org/10.1126/science.1087393

Roberts, D., Howard, W., Moy, A., Roberts, J., Trull, T., Bray, S., & Hopcroft, R. (2011). Interannual pteropod variability in sediment traps deployed above and below the aragonite saturation horizon in the Sub-Antarctic Southern Ocean. *Polar Biology*, *34*(11), 1739–1750. https://doi.org/10.1007/s00300-011-1024-z

Salisbury, J., Green, M., Hunt, C., & Campbell, J. (2008). Coastal acidification by rivers: A threat to shellfish? *Eos, Transactions of the American Geophysical Union*, *89*(50), 513–528. https://doi.org/10.1029/2008EO500001

Schouten, S., van Kaam-Peters, H. M. E., Rijpstra, W. I. C., Schoell, M., & Sinninghe Damsté, J. S. (2000). Effects of an oceanic anoxic event on the stable carbon isotopic composition of early toarcian carbon. *American Journal of Science*, *300*(1), 1–22. https://doi.org/10.2475/ajs.300.1.1

Silva, N. (2008). Dissolved oxygen, pH, and nutrients in the austral Chilean channels and fjords. In N. Silva & S. Palma (Eds.), *Progress in the oceanographic knowledge of Chilean interior waters, from Puerto Montt to Cape Horn*, *Comité Oceanográfico Nacional* (pp. 37–43). Valparaíso, Chile: Pontificia Universidad Católica de Valparaíso.

Silva, N., & Vargas, C. A. (2014). Hypoxia in Chilean Patagonian fjords. *Progress in Oceanography*, *129*, 62–74. https://doi.org/10.1016/j.pocean.2014.05.016

Silva, N., Vargas, C. A., & Prego, R. (2011). Land-ocean distribution of allochthonous organic matter in the surface sediments of the Chiloé and Aysén interior seas (Chilean Northern Patagonia). *Continental Shelf Research*, *31*(3-4), 330–339. https://doi.org/10.1016/j.csr.2010.09.009

Smith, R. W., Bianchi, T. S., Allison, M., Savage, C., & Galy, V. (2015). High rates of organic carbon burial in fjord sediments globally. *Nature Geoscience*, *8*(6), 450–453. https://doi.org/10.1038/ngeo2421

Strub, P. T., Mesias, J., Montecino, V., Rutllant, J., & Salinas, S. (1998). Coastal ocean circulation off western South America. In A. R. Robinson & K. H. Brink (Eds.), *The sea* (Vol. 11, pp. 273–313). New York: Wiley.

Torres, R., Frangópulos, M., Hamamé, M., Montecino, V., Maureira, C., Pizarro, G., … Blanco, J. L. (2011). Nitrate to silicate ratio variability and the composition of microphytoplankton blooms in the inner-fjord of Seno Ballena (Strait of Magellan, 54°S). *Continental Shelf Research*, *31*(3-4), 244–253. https://doi.org/10.1016/j.csr.2010.07.014

Torres, R., Silva, N., Reid, B., & Frangopulos, M. (2014). Silicic acid enrichment of subantarctic surface water from continental inputs along the Patagonian archipielago interior sea (41–56°S). *Progress in Oceanography*, *129*, 50–61. https://doi.org/10.1016/j.pocean.2014.09.008

Turner, E. R., Qureshi, N., Rabalais, N. N., Dortch, Q., Justic, D., Shaw, R. F., & Cope, J. (1988). Fluctuating silicate:nitrate ratios and coastal plankton food webs. *Proceedings of the National Academy of Sciences of the United States of America*, *95*, 13,048–13,051.

Tyson, R. V. (1995). Bulk geochemical characterizations and classification of organic matter: stable carbon isotopes ($\delta^{13}C$). In *Sedimentary organic matter* (pp. 395–416). London: Chapman & Hall.

Valdenegro, A., & Silva, N. (2003). Caracterización oceanográfica física y química de la zona de cana- les y fiordos australes de Chile entre el estrecho de Magallanes y cabo de Hornos (CIMAR 3 Fiordos). *Ciencia e Tecnologia Marketing*, *26*(2), 19–60.

van Breugel, Y., Schouten, S., Paetzel, M., Nordeide, R., & Sinninghe Damsté, J. S. (2005). The impact of recycling of organic carbon on the stable carbon isotopic composition of dissolved inorganic carbon in a stratified marine system (Kyllaren fjord, Norway). *Organic Geochemistry*, *36*(8), 1163–1173. https://doi.org/10.1016/j.orggeochem.2005.03.003

Vargas, C. A., Martínez, R. A., González, H. E., & Silva, N. (2008). Contrasting trophic interactions of microbial and copepod communities in a fjord ecosystem, Chilean Patagonia. *Aquatic Microbial Ecology*, *53*(2), 227–242. https://doi.org/10.3354/ame01242

Vargas, C. A., Martínez, R. A., San Martín, V., Aguayo, M., Silva, N., & Torres, R. (2011). Allochthonous subsidies of organic matter across a lake–river–fjord landscape in the Chilean Patagonia: Implications for marine zooplankton in inner fjord areas. *Continental Shelf Research*, *31*(3-4), 187–201. https://doi.org/10.1016/j.csr.2010.06.016

Yamamoto-Kawai, M., McLaughlin, F. A., Carmack, E. C., Nishino, S., & Shimada, K. (2009). Aragonite undersaturation in the Arctic Ocean: Effects of ocean acidification and sea ice melt. *Science*, *326*(5956), 1098–1100. https://doi.org/10.1126/science.1174190